Cement 3 (2021) 100004

Contents lists available at ScienceDirect

Cement

journal homepage: www.elsevier.com/locate/cement

The effective volumes of waters of crystallization & the thermodynamics of cementitious materials

Leslie Glasser

Curtin Institute for Computation, Discipline of Chemistry, Curtin University, GPO Box U1987, Perth, WA 6845, Australia

ARTICLE INFO

Keywords:
Calcium-silicate-hydrates (C-S-H)
Hydration products
Thermodynamic calculations
Calcium aluminate cement
Portland cement

ABSTRACT

Hydrates are significant components of cements and concrete. We examine the effective volumes of waters of crystallization for these materials, where the "effective volumes" are the difference per water molecule between the formula volume of the hydrate and of its parent anhydrate. These effective volumes cover a small range around 15 cm^3 mol^{-1} (≅ 23 $Å^3$ per water molecule), unlike the wider range for general inorganic materials.

We also examine the thermodynamic properties of the cementitious phase, which follow the generally observed correlation of relating to their molar volumes. We establish "effective" additive oxide parameters for enthalpy and for molar volume, which are useful in confirming experimental values and in predicting as-yet undetermined values. Their Debye temperatures approximate to 600 K; this Debye temperature is well above ambient temperature and suggests that the vibrational modes of these cementitious phases are only partially excited and that the materials are hard. Ferrate-containing materials generally have a lower Debye temperature (~273 K) implying that they may be softer than other cementitious materials.

These observations may be useful in checking for errors in data and anomalies in behavior among related cementitious materials.

1. Introduction

Molecules under ambient conditions are generally regarded as incompressible, having fixed atomic radii [1] but with some flexibility of bond lengths and angles and possible conformational changes resulting from rotation about bonds. When this incompressible water is introduced into a crystal structure, the volume of that structure is expected to increase by approximately the volume of the water molecule, subject to possible adjustments in the conformation of the parent anhydrate, which may add or subtract from the volume, effects from hydrogen bonding and other interactions, and filling of voids. The volumes referenced are experimental values from measured density or structural values from X-ray crystallography. We term the difference in volume per water of crystallization between hydrate and parent the "effective volume" of the water of crystallization;

We have recently examined effective volumes for general ionic solids [2], for non-ionic pharmaceutical systems [3], and for general organics [4]. For general ionic solids, we observe that the effective volumes extend up to a seeming upper limit of about 30 $Å^3$ per H_2O molecule (≅ 18 cm^3 mol^{-1}), which corresponds to the formula volume of liquid water under ambient conditions (but less than the 32 $Å^3$ observed for the hydrogen-bonded structure of hexagonal ice) and down towards zero as a consequence of the hydration water occupying voids in the anhydrate, together with possible conformational re-arrangements.

In the current paper we examine the effective volumes of waters of crystallization in the structures of calcium aluminate and other hydrates as found in cements and concrete, and also examine some accompanying thermodynamic correlations.

These observations may be useful in checking for errors in data and anomalies [5] in behavior among related cementitious materials.

2. Data collection

Lothenbach, et al. [6] summarize cementitious hydrate data in the *Cemdata18* cement database while Blanc, et al., [7,8] report on their *Thermoddem* database. *Cemdata18* reports thermodynamic data (Gibbs energy, *G;* enthalpy, *H;* entropy, *S;* heat capacity, C_p; and molar volume, V_m) at 25 °C for 41 calcium aluminate hydrates of slightly differing composition. *Thermoddem* deals with the chemical systems SO_3–Al_2O_3–CaO–CO_2–Cl–H_2O and SiO_2–Al_2O_3–CaO–H_2O, including iron- and magnesium-bearing phases. In Supplementary Table S1 we list from *Cemdata18* the numbers of waters of crystallization, $n(H_2O)$, the reported molar volumes, V_m, the entropy, *S*, and the heat capacity, C_p, extracted from the database. The Table is divided into two groups,

E-mail address: l.glasser@curtin.edu.au

https://doi.org/10.1016/j.cement.2021.100004
Received 5 September 2020; Received in revised form 17 January 2021; Accepted 19 January 2021
Available online 23 January 2021

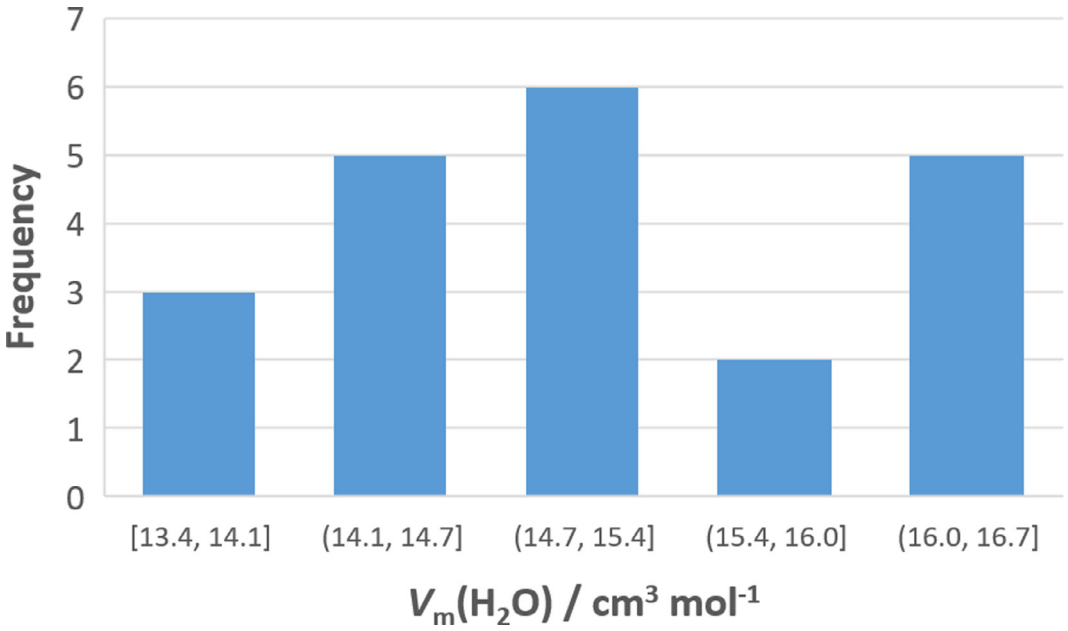

Fig. 1. Histogram of $V_m(H_2O)$ / cm^3 mol^{-1} for 21 AFm phases,[6] using data from Table S1, with a mean value of 15.1 ± 0.9 cm^3 mol^{-1} (omitting outlier C_2ASHn with $V_m(H_2O) = 1.21$ cm^3 mol^{-1}; cf. legend to Fig. 2).

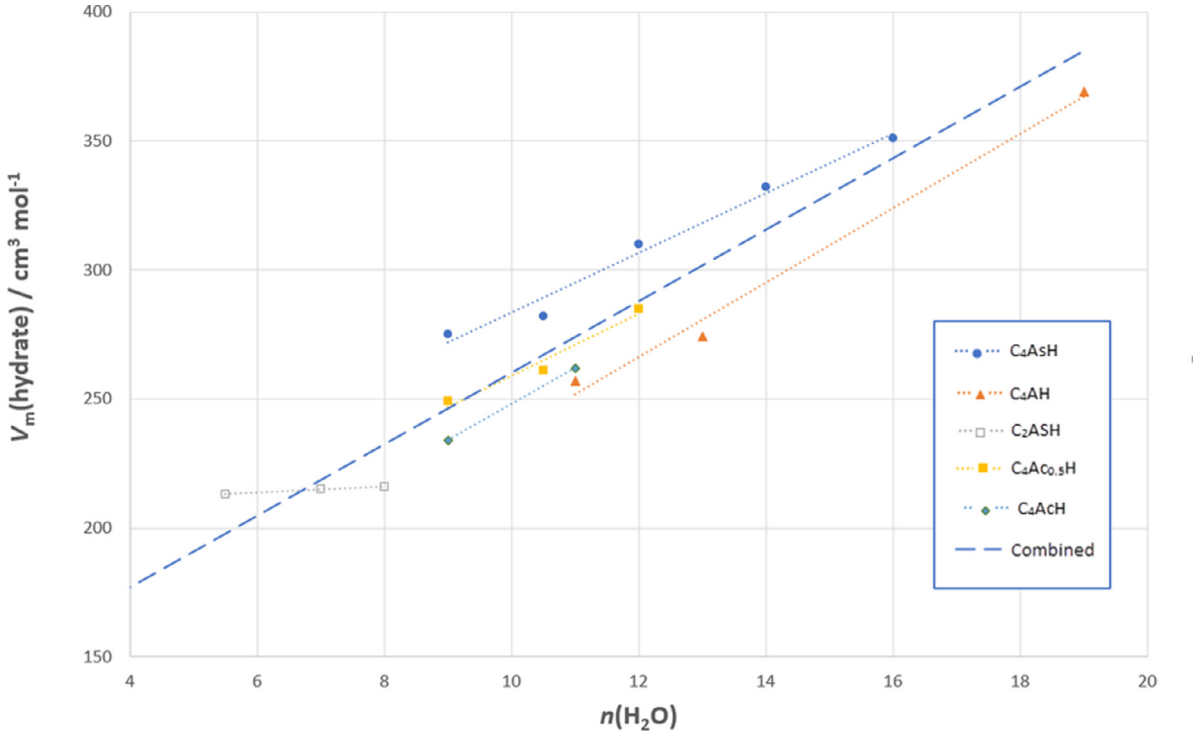

Fig. 2. Molar volume, V_m(hydrate) / cm^3 mol^{-1}, versus $n(H_2O)$ for AFm phases,[6] using data from Table S1.
C_4AsHn: blue circle (●) $V_m = 11.53n + 168.2$, $R^2 = 0.98$;; $C_4Ac_{0.5}Hn$: yellow square(■) $V_m = 12n + 139$, $R^2 = 1$; C_4AcHn: green diamond (◆) $V_m = 14n + 108$, $R^2 = 1$; C_4AHn: orange triangle (▲) $V_m = 14.42n + 93.3$, $R^2 = 0.99$; C_2ASHn: open square (□) $V_m = 1.21n + 206.4$, $R^2 = 0.99$; Combined AFm data, blue broken line, $V_m = 13.9n + 121.4$, $R_2 = 0.73$, $N = 27$. (For interpretation of the references to color in this figure legend, the reader is referred to the web version of this article.)

Al_2O_3-Fe_2O_3 mono (labelled AFm, of general simplified composition $3CaO{\cdot}(Al,Fe)_2O_3{\cdot}CaSO_4{\cdot}nH_2O$) and Al_2O_3-Fe_2O_3 tri (labelled AFt, of general simplified composition $3CaO{\cdot}(Al,Fe)_2O_3{\cdot}3CaSO_4{\cdot}nH_2O$). Within each group we have separated sets (italicized) with the same chemical formula and differing numbers of water of crystallization. These data sets are plotted in Figs. 1–3. Cementitious phase data is also available from the current *Thermochimie* database [9].

3. Effective volumes

Effective volumes are determined as the difference between the experimental molar volumes of hydrate and anhydrate parent, divided by the number of water molecules in the hydrate. Experience [2] suggests that the resultant effective volumes may be relied upon to the extent of 1–2 Å^3 in general (~5%), down to 0.1 Å^3 when the data for the hy-

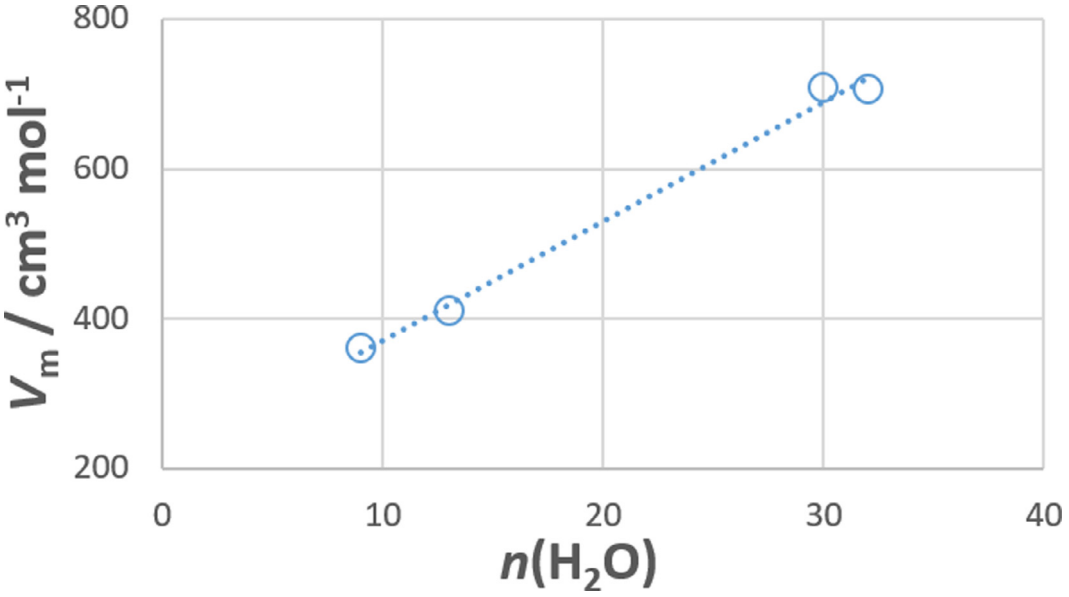

Fig. 3. Molar volume, V_m(hydrate) / cm^3 mol^{-1}, versus $n(H_2O)$ for AFt phases,[6] using data from Table S1. For $C_6As_3H_{32}$, $C_6As_3H_{30}$, $C_6As_3H_{13}$ and $C_6As_3H_9$: $V_m = 15.9n + 212.3$, $R^2 = 0.99$.

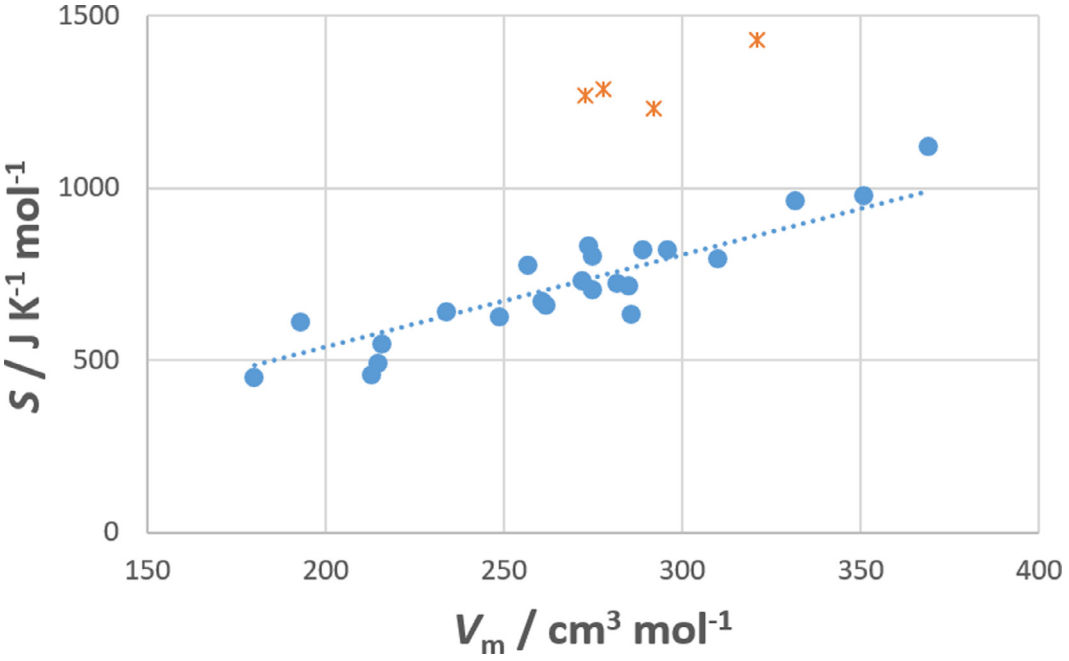

Fig. 4. Plot of S/J K^{-1} mol^{-1} versus molar volume, V_m/cm^3 mol^{-1} for AFm hydrates,[6] constrained to zero intercept – that is, the entropy is constrained to zero when the molar volume is zero. The fitted slope is 2.69 ± 0.05 J K^{-1} cm^{-3}, $R^2 = 0.99$. The outlier group of materials shown with star symbols all contain ferrates and have relatively large entropies: $C_4Fc_{0.5}H_{10}$, C_4FcH_{12}, C_4FsH_{12} and $C_4FCl_2H_{10}$.

drate and anhydrate pair are both reported by the same experimental group.

There is, inevitably, a much smaller dataset for these oxide-based cementitious materials than for the general set of ionic solids [2] so that the data does not encompass the full possible range of $n(H_2O)$ values. Instead, while it stretches across a range of values, there are only one or a few representative examples of each. The histogram for the AFm phases in Fig. 1 shows that the effective volumes of water of crystallization cover the range from about 13–17 cm^3 mol^{-1} with a mean value 15.1 ± 0.9 cm^3 mol^{-1}. This is rather smaller than the mean value of 24 cm^3 mol^{-1} for a wide range of ionic solids [2].

Since there are multiple hydrates of some of the AFm phases, we can investigate the effective volumes for each individually. In Fig. 2, there is plotted the volume versus hydration number for the five individual phases C_4ASHn, C_4AHn, $C_4Ac_{0.5}Hn$, C_4AcHn and C_2ASHn together with the combined data for the full set of AFm phases in Table S1. From the slopes of the fitted linear equations, we see that the effective volumes of the hydration waters are very similar at 12, 14, 12 and 14 cm^3 mol^{-1},

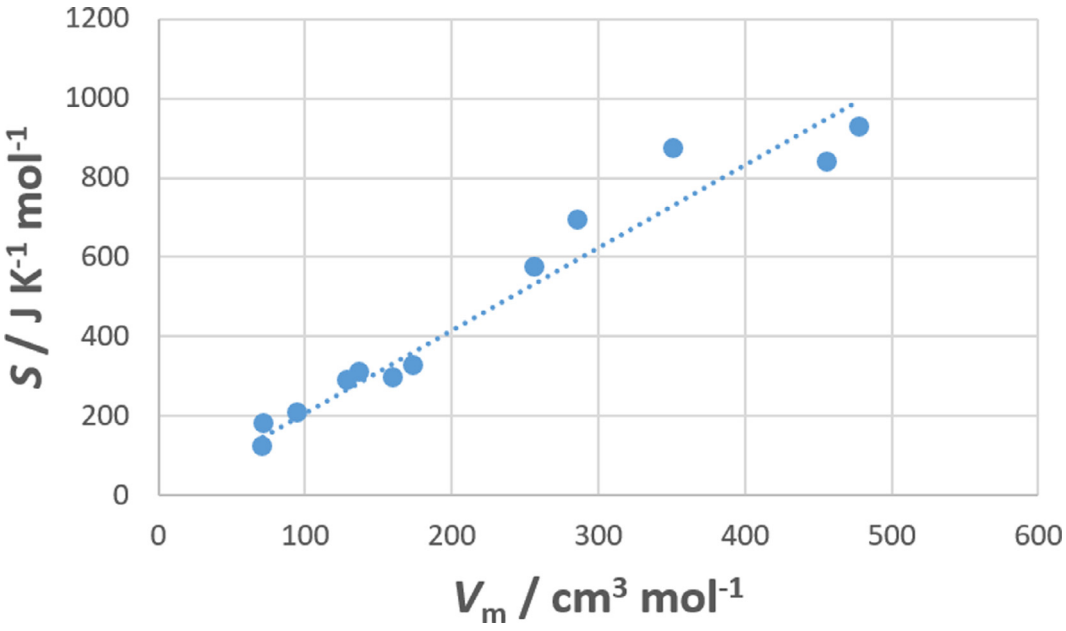

Fig. 5. Plot of S/J K^{-1} mol^{-1} versus molar volume, V_m/cm^3 mol^{-1} for calcium silicate mineral hydrates from Table S2.[6] The fitted slope, constrained to zero intercept, is 2.08 ± 0.08 J K^{-1} cm^{-3}, $R^2 = 0.99$. Compare Fig. 4 for AFm hydrates which has a slope 2.69 ± 0.05 J K^{-1} cm^{-3}.

respectively, but 1.2 cm^3 mol^{-1} for C_2ASHn. This discrepancy is further considered in Section 5 (entitled "Additive Fitting Parameters"). For AFt phases (Fig. 3), the slope of the fitted linear equation yields an effective volume for water of crystallization of 16 cm^3 mol^{-1}.

The intercepts for the selected groups of these equations are also informative, providing an approximate measure of the mean effective volume of the anhydrate as contained in the hydrate. In the case of the C_4ASHn phases, the anhydrate volume is reported as 122 cm^3 mol^{-1} while the calculated intercept is considerably larger at 168 cm^3 mol^{-1}. From Fig. 2 it can be observed that the slope is too small relative to the others shown, suggesting that the data for the C_4ASHn hydrates are inconsistent, and worthy of further investigation.

4. Thermodynamic correlations

Thermodynamics provides information for fundamental understanding of the relations between materials [10] as also for cement science [11–13]. It has earlier [14] been established for both inorganic hydrates and their anhydrates that there is a strong correlation between entropy and molar volume under ambient conditions. Fig. 4 provides evidence that a similar correlation occurs for cementitious hydrates, with a fitted linear equation with intercept constrained to zero. The fitted slope of 2.69 J K^{-1} cm^{-3} may be converted to comparable molecular units by multiplication by $N_A/[10^{21}\ \text{nm}^3/\text{cm}^3] = 6.022 \times 10^{23}/10^{21} = 602.2$, where N_A is Avogadro's Constant. Thus 2.69 J K^{-1} cm^{-3} corresponds to 1 620 J K^{-1} nm^{-3} (H_2O molecule)$^{-1}$. This entropy value may be compared with the recent essentially identical value [2] for the general class of ionic hydrates of 1 637 J K^{-1} nm^{-3} (H_2O molecule)$^{-1}$. Ghazizadeh, et al. [15] have also recently performed a thorough analysis of estimation of standard molar entropy of cement hydrates and clinker minerals by this volume-based method.

In Supplementary Table S2, we collect some relevant data for calcium silicate mineral hydrates from the *Thermoddem* database which is plotted in Fig. 5.

Another observed thermodynamic correlation for hydrated mineral calcium aluminates (Fig. 6) is that between entropy and heat capacity, which are often observed to be nearly equal and related through the Debye equation [16].

The slopes $C_p/S = 1.10$ of the fitted lines agree closely with the value of 1.09 earlier noted for a wider range of similar materials (in Fig. 4 of the relevant reference) [16]. One may obtain the corresponding Debye temperature, $\Theta_D \cong 600$ K, by using the tabulation in the Supplementary File accompanying that publication. This Debye temperature is well above ambient temperature and suggests that the vibrational modes of these cementitious phases are only partially excited and that they are hard materials. By contrast, soft inorganic materials, such as CsI, have low Debye temperatures (113 K) with strongly excited vibrational modes.

An unexpected observation is that the C_p/S ratio for ferrate-containing materials is generally small for both AFm and AFt phases (but with some exceptions - see Supplementary Table S1), with an average value of about 0.7. This implies [16] a smaller Debye temperature ($\Theta_D \cong 273$ K) and softer materials than those with the larger C_p/S ratio.

5. Additive fitting parameters: "effective" oxide contributions to the hydrate

As the standard simple cement notation suggests, the chemical formulae of cementitious materials can be described in additive terms of component oxides. It is of interest to investigate how far this concept can be extended to additive terms for their thermodynamic properties, as has earlier been explored for inorganic systems [17]. We have performed such analyzes for cementitious materials for formation enthalpy, $\Delta_f H$, entropy, formation Gibbs energy, $\Delta_f G$, heat capacity, C_p, and molar volume, V_m.

The results for formation enthalpy have proven to be very satisfactory with small errors, as reported below, but entropy and the related heat capacity and Gibbs energy provide rather poor additivity (and so are not reported further) while molar volume does yield informative results.

The optimization process in Microsoft Excel involves initially listing the oxide components with an arbitrary value which will subse-

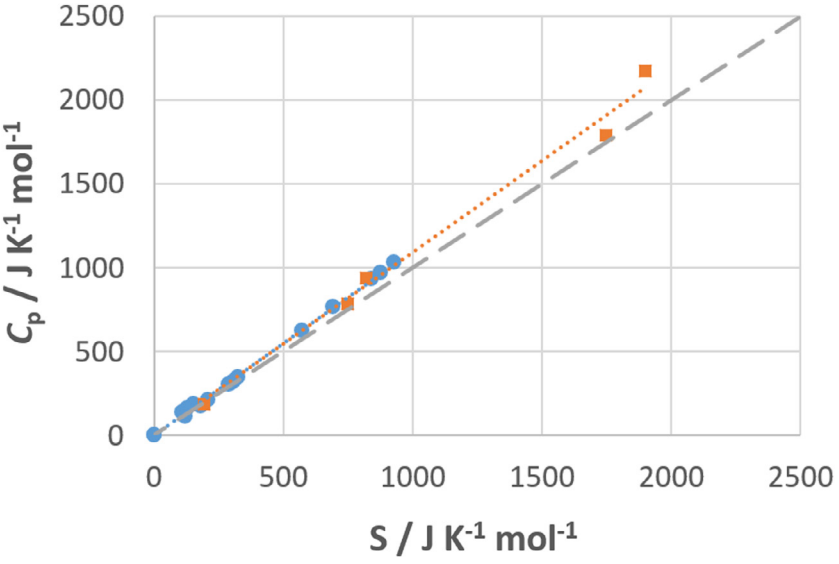

Fig. 6. Heat capacity, C_p/J K^{-1} mol^{-1}, versus entropy, S/J K^{-1} mol^{-1} for hydrated mineral calcium silicates[7] from Table S2 and from Supplementary Table S3 (orange squares).[8] The diagonal broken line has a 1:1 slope, representing equality of C_p and S. The slopes of both fitted trendlines (each with intercepts constrained to zero) are $C_p/S = 1.10$ with $R^2 = 0.99$. (For interpretation of the references to color in this figure legend, the reader is referred to the web version of this article.)

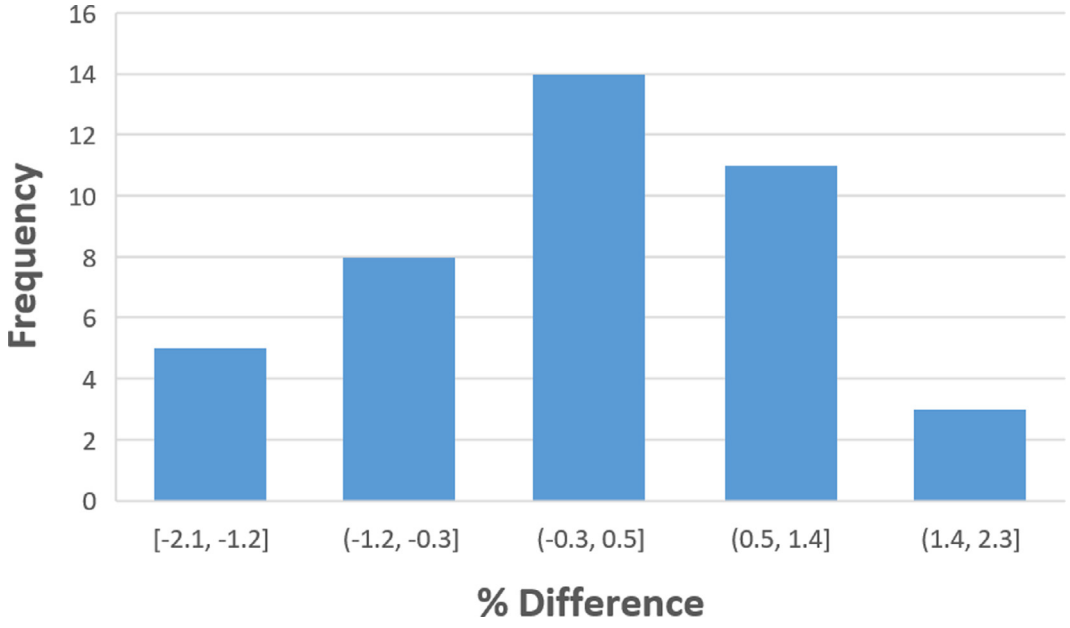

Fig. 7. Histogram of the percentage difference between the reported enthalpy[6] and the sum of the optimized additive terms for the 41 AFTm and AFt phases from Table 1. The differences range between 2.3% and −2.1%, with a mean difference of 0 ± 1%.

quently be optimized (where available, the relevant thermodynamic property of the oxide may conveniently serve as the initial value - see Table 1 for an example of the finalized Table). The cement phases, together with their values of the relevant reported thermodynamic quantity, are listed separately in a table together with the sum formula for the phase using the currently optimized oxide values. For example, for C_4AH_{19}, the Excel formula is: "= C*4 + A + H*19″ where the named Excel symbols return the current oxide value. The sum of the squares of the differences ("ssqdiff") between the reference value and the current sum formula value is listed in a cell (using the Excel function SUMXMY2). Optimization is performed using the Excel Solver function, which minimizes the "ssqdiff" values by adjusting the initial arbitrary estimates. The resultant optimized values may be considered to be the "effective" thermodynamic contributions of the oxide terms to the hydrate. It will be noted in Table 1 that these "effective" terms

Table 1
Optimized additive unit formation enthalpies, compared with reference standard formation enthalpies[6] (at 25 °C) of the corresponding oxides.

Oxide	Cement Symbol	Optimized Unit Enthalpy	Reference $\Delta_f H$ /kJ mol^{-1}	Ratio optimized/ reference
Al_2O_3	A	−1523.58	−1675.69	0.91
CaO	C	−730.74	−634.92	1.15
Fe_2O_3	F	−435.20	−824.78	0.53
H_2O	H	−300.52	−285.83	1.05
SiO_2	S	−977.92	−910.86	1.07
CO_2	c	−564.16		
SO_2	s	−637.64		
Cl	Cl	−81.59		
NO_2	noa	−20.71		
NO_3	nob	−133.80		

Table 2
Reference[6] and summed standard enthalpies of formation at 25 °C of cementitous AFm and AFt phases based upon the optimized additive oxide contribution terms listed in Table 1.

Afm-phases (cement notation)	Reference $\Delta_f H$ /kJ mol^{-1}	H_Sum	% Difference
C_4AH_{19}	−10017.9	−10156.3	−1.4
C_4AH_{13}	−8262.4	−8353.2	−1.1
C_4AH_{11}	−7656.6	−7752.2	−1.2
$C_2AH_{7.5}$	−5277.5	−5238.9	0.7
CAH_{10}	−5288.2	−5259.5	0.5
$C_4Ac_{0.5}H_{12}$	−8270	−8334.8	−0.8
$C_4Ac_{0.5}H_{10.5}$	−7813.3	−7884.0	−0.9
$C_4Ac_{0.5}H_9$	−7349.7	−7433.3	−1.1
C_4AcH_{11}	−8250	−8316.4	−0.8
C_4AcH_9	−7618.6	−7715.3	−1.3
C_4AsH_{16}	−9930.5	−9892.4	0.4
C_4AsH_{14}	−9321.8	−9291.4	0.3
C_4AsH_{12}	−8758.6	−8690.4	0.8
$C_4AsH_{10.5}$	−8311.9	−8239.6	0.9
C_4AsH_9	−7845.5	−7788.8	0.7
C_2ASH_8	−6360	−6367.1	−0.1
C_2ASH_7	−6066.8	−6066.6	0.0
$C_2ASH_{5.5}$	−5603.4	−5615.8	−0.2
$C_4As_{0.5}ClH_{12}$	−8472	−8453.1	0.2
$C_4ACl_2H_{10}$	−7604	−7614.9	−0.1
$C_4A(NO_3)_2H_{10}$	−7719.3	−7719.3	0.0
$C_4A(NO_2)_2H_{10}$	−7493.1	−7493.1	0.0
C_4FH_{13}	−7435	−7264.9	2.3
$C_4Fc_{0.5}H_{10}$	−6581	−6645.4	−1.0
C_4FcH_{12}	−7485	−7528.5	−0.6
C_4FsH_{12}	−7663	−7602.0	0.8
$C_4FCl_2H_{10}$	−6528	−6526.5	0.0
$C_6As_3H_{32}$	−17535.0	−17437.5	0.6
$C_6As_3H_{30}$	−16950.2	−16836.4	0.7
$C_6As_3H_{13}$	−11530.3	−11727.6	−1.7
$C_6As_3H_9$	−10643.7	−10525.6	1.1
$C_6Ac_3H_{30}$	−16792.0	−16616.0	1.0
$C_6F_2s_3H_{32}$	−16600.0	−16784.3	−1.1
C_3ScsH_{15}	−8700.0	−8879.7	−2.1
C_3AH_6	−5537.3	−5518.9	0.3
$C_3AS_{0.41}H_{5.18}$	−5699.0	−5673.4	0.4
$C_3AS_{0.84}H_{4.32}$	−5847.0	−5835.5	0.2
C_3FH_6	−4518.0	−4430.5	1.9
$C_3FS_{0.84}H_{4.32}$	−4823.0	−4747.1	1.6
$C_3A_{0.5}F_{0.5}S_{0.84}H_{4.32}$	−5335.0	−5291.3	0.8
$C_3FS_{1.34}H_{3.32}$	−4994.0	−4935.5	1.2

are not dissimilar from their standard reference values. Of course, the optimized effective values are dependent on the particular set of data supplied.

5.1. Enthalpy

Table 2 lists the optimized results for the enthalpies of the AFm and AFt cement phases while Fig. 7 is a histogram of the percentage errors. The histogram shows that these errors are generally of the order of 1% and symmetrically distributed. It will also be noted that there are a few entries where the "% Difference" is listed as 0% (for example, $C_4FCl_2H_{10}$). These are where this is the only entry containing an example of a particular sum term ("Cl" in this case), when Solver is able to adjust that sum term for an exact fit.

5.2. Molar volume

Table 3 lists the optimized results for the enthalpies of 38 AFm and AFt cement phases while Fig. 8 is a histogram of the percentage errors.

Table 3
Optimized additive molar volumes, compared with reference molar volumes of the corresponding oxides.

	Symbol	Optimized Unit Volume	Reference V / cm^3 mol^{-1}	Ratio optimized/reference
Al_2O_3	A	15.13	25.72	0.59
CaO	C	18.41	16.79	1.10
Fe_2O_3	F	19.02	30.47	0.62
H_2O	H	15.18	19.65	0.77
SiO_2	S	7.76	23.11	0.34
CO_2	c	20.31		
SO_2	s	32.81		
Cl	Cl	14.59		
NO_2	noa	17.19		
NO_3	nob	27.69		

Table 4
Effective molar volumes of water of crystallization for AFm phases, based on known experimental molar volumes of the hydrate[6] and summed volumes (using data from Table 3) of the anhydrate. The summed anhydrate volume for the problematic C2AS is 82 cm^3 mol^{-1}.

			V / cm^3 mol^{-1}	
AFm-phases	$n(H_2O)$	V_m (Hydrate)	V_m (Anhydrate Sum)	$\Delta V(H_2O)$ from sum
C_4AH_{19}	19	369	*93*	15
C_4AH_{13}	13	274	*93*	14
C_4AH_{11}	11	257	*93*	15
$C_2AH_{7.5}$	7.5	180	*59*	16
CAH_{10}	10	193	*43*	15
$C_4Ac_{0.5}H_{12}$	12	285	*103*	15
$C_4Ac_{0.5}H_{10.5}$	10.5	261	*103*	15
$C_4Ac_{0.5}H_9$	9	249	*103*	16
C_4AcH_{11}	11	262	*113*	14
C_4AcH_9	9	234	*113*	13
C_4AsH_{16}	16	351	*122*	14
C_4AsH_{14}	14	332	*122*	15
C_4AsH_{12}	12	310	*122*	16
$C_4AsH_{10.5}$	10.5	282	*122*	15
C_4AsH_9	9	275	*122*	17
C_2ASH_8	8	216	*82*	17
C_2ASH_7	7	215	*82*	19
$C_2ASH_{5.5}$	5.5	213	*82*	24
$C_4As_{0.5}ClH_{12}$	12	289		
$C_4ACl_2H_{10}$	10	272	*128*	14
$C_4A(NO_3)_2H_{10}$	10	296	*142*	15
$C_4A(NO_2)_2H_{10}$	10	275		
C_4FH_{13}	13	286	*98*	14
$C_4Fc_{0.5}H_{10}$	10	273	*108*	17
C_4FcH_{12}	12	292	*118*	15
C_4FsH_{12}	12	321	*127*	16

If the C_2ASHn phases are removed from the volume data (on account of the anomalous behavior already noted in Fig. 2) a relatively symmetrical distribution of the remaining 38 data items is obtained with errors of 0.0 ± 8 cm^3 mol^{-1}. The optimized molar volume table for 38 AFTm and AFt phases as summarized in the histogram of Fig. 8 exhibits a broad distribution of errors, but the optimized values listed in Table 3 above may still usefully be applied in order to estimate the molar volumes of otherwise unknown phases as may be found in Section 5.2.1.

5.2.1. Molar volume estimations

The optimized oxide volume parameters may be used to estimate volumes for the anomalous C_2ASHn phases, namely: V / cm^3 mol^{-1} for C_2ASH_8: 181.2 (cf. *Cemdata* volume: 216); for C_2ASH_7: 166.0 (cf. *Cemdata* 215); for $C_2ASH_{5.5}$: 143.2 (cf. *Cemdata* 213). This yields a more credible linear fit of $V_m(C_2ASHn) = 15.18n + 59.72$ with the intercept thus yielding a volume of 60 cm^3 mol^{-1} for the anhydrous C_2AS com-

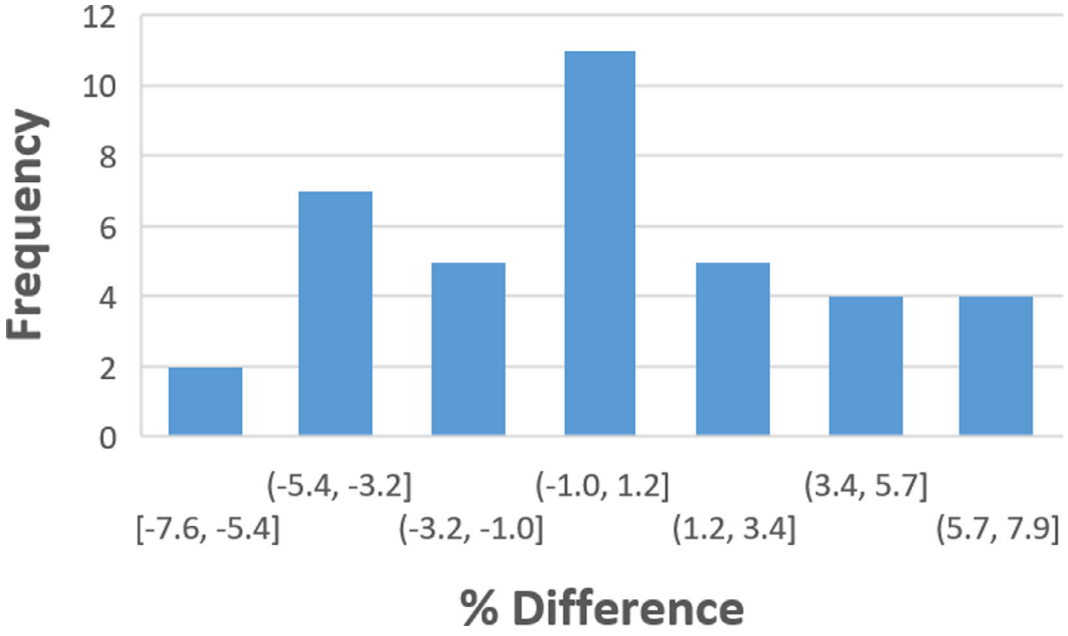

Fig. 8. Histogram of the percentage difference between the reported molar volume[6] and the sum of the optimized additive terms for 38 AFTm and AFt phases. The maximum differences are ± 8%, with a mean difference of 0.0 ± 3.9%.

pared with the dubious extrapolated experimental value of 206.4 cm^3 mol^{-1} (noted as the intercept in the Fig. 2 legend: $V_m = 1.21n + 206.4$, R^2=0.99).

The molar volumes of the anhydrates are not generally known. The optimized oxide volume data of Table 3 provides a method for finding the volumes of the anhydrates in addition to the values derived from intercepts. As for C_2ASHn above, the data in Table 3 may be summed in order to estimate anhydrate volumes (Table 4). The effective volume per water molecule is then obtained from [V_m(hydrate) - V_m (anhydrate)]/n(H_2O), and is listed in the final column of Table 4. The mean effective volume is 15.7 ± 2.2 cm^3 mol^{-1} which differs little from the raw data in Table S1, which yields 15.1 ± 0.9 cm^3 mol^{-1} (as shown in Fig. 1). This agreement provides confirmation of the reliability of the two procedures.

6. Conclusions

For the listed hydrated cementitious materials, the effective volumes of waters of crystallization cover a small range around 15 cm^3 mol^{-1} of added water, unlike the wider range for general hydrated inorganic materials. This results from working with the limited class of cementitious materials. The thermodynamic behavior, however, does tend to follow the generally observed pattern; in particular, some thermodynamic properties may be closely correlated with the molar volumes of the hydrated cementitious materials.

Optimized additive oxide component values have been developed for enthalpies and (rather less accurately) for molar volumes. An example of volume estimation using this data is reported for the C_2ASHn phases, and is extended to estimation of the molar volumes of the anhydrates.

Debye temperatures are generally well above ambient, at 600 K, hence vibrational modes are only slightly excited and the materials are hard. Ferrate-containing cementitious materials generally have Debye temperatures near ambient and so may be softer.

These observations may be useful in checking for errors in data and for anomalies in behavior among related cementitious materials, and may even be used for predicting as-yet undetermined values as demonstrated for the anhydrate molar volumes.

Declaration of Competing Interest

The authors declare that they have no known competing financial interests or personal relationships that could have appeared to influence the work reported in this paper.

Funding

This research did not receive any specific grant from funding agencies in the public, commercial, or not-for-profit sectors.

Supplementary materials

Supplementary material associated with this article can be found, in the online version, at doi:10.1016/j.cement.2021.100004.

References

[1] D.W.M. Hofmann, Fast estimation of crystal densities, Acta Crystallogr. B 58 (2002) 489–493.
[2] L. Glasser, Effective volumes of waters of crystallization: ionic Systems, Cryst. Growth Des. 19 (2019) 3397–3401.
[3] L. Glasser, The effective volumes of waters of crystallization: non-ionic pharmaceutical systems, Acta Crystallogr. B 75 (2019) 784–787.
[4] L. Glasser, The effective volumes of waters of crystallization: general organic solids, Acta Crystallogr. B 76 (2020) 650–653.
[5] W. Clegg, Distortions, deviations and alternative facts: reliability in crystallography, IUCrJ 8 (2021) 4–11.
[6] B. Lothenbach, D.A. Kulik, T. Matschei, M. Balonis, L. Baquerizo, B. Dilnesa, G.D. Miron, R.J. Myers, Cemdata18: a chemical thermodynamic database for hydrated Portland cements and alkali-activated materials, Cem. Concr. Res. 115 (2019) 472–506.
[7] P. Blanc, X. Bourbon, A. Lassin, E.C. Gaucher, Chemical model for cement-based materials: temperature dependence of thermodynamic functions for nanocrystalline and crystalline C–S–H phases, Cem. Concr. Res. 40 (2010) 851–866.
[8] P. Blanc, X. Bourbon, A. Lassin, E.C. Gaucher, Chemical model for cement-based materials: thermodynamic data assessment for phases other than C–S–H, Cem. Concr. Res. 40 (2010) 1360–1374.
[9] **Consortium Andra - Ondraf/Niras - RWM Thermochimie - cementitious phases**. https://www.thermochimie-tdb.com/ (Accessed January 2021).
[10] L. Glasser, H.D.B. Jenkins, Predictive thermodynamics for ionic solids and liquids, Phys. Chem. Chem. Phys. 18 (2016) 21226–21240.
[11] D. Damidot, B. Lothenbach, D. Herfort, F.P. Glasser, Thermodynamics and cement science, Cem. Concr. Res. 41 (2011) 679–695.

[12] B. Lothenbach, M. Zajac, Application of thermodynamic modelling to hydrated cements, Cem. Concr. Res. 123 (2019) 105779.
[13] B. Ma, B. Lothenbach, Thermodynamic study of cement/rock interactions using experimentally generated solubility data of zeolites, Cem. Concr. Res. (2020) 135.
[14] H.D.B. Jenkins, L. Glasser, Standard absolute entropy, S_{298}°, values from volume or density. 1. Inorganic materials, Inorg. Chem. 42 (2003) 8702–8708.
[15] S. Ghazizadeh, T. Hanein, J.L. Provis, T. Matschei, Estimation of standard molar entropy of cement hydrates and clinker minerals, Cem. Concr. Res. 136 (2020) 106188.
[16] L. Glasser, Ambient heat capacities and entropies of ionic solids: a unique view using the Debye equation, Inorg. Chem. 52 (2013) 6590–6594.
[17] L. Glasser, Single-ion values for ionic solids of both formation enthalpies, $\Delta_f H(298)_{ion}$, and Gibbs formation energies, $\Delta_f G(298)_{ion}$, Inorg. Chem. 52 (2013) 992–998.